symmetry

MDPI

Article

A Shift-Dependent Measure of Extended Cumulative Entropy and Its Applications in Blind Image Quality Assessment

Saeid Tahmasebi [1], Ahmad Keshavarz [2], Maria Longobardi [3,*] and Reza Mohammadi [4]

1 Department of Statistics, Persian Gulf University, Bushehr 7516913817, Iran; tahmasebi@pgu.ac.ir
2 Department of Electrical Engineering and the ICT Research Institute, Persian Gulf University, Bushehr 7516913817, Iran; a.keshavarz@pgu.ac.ir
3 Dipartimento di Matematica e Applicazioni Universita di Napoli Federico II, I-80126 Napoli, Italy
4 Department of Operation Management, Amsterdam Business School, University of Amsterdam, 1018 TV Amsterdam, The Netherlands; a.mohammadi@uva.nl
* Correspondence: maria.longobardi@unina.it

Received: 23 December 2019; Accepted: 18 February 2020; Published: 23 February 2020

check for updates

Abstract: Recently, Tahmasebi and Eskandarzadeh introduced a new extended cumulative entropy (ECE). In this paper, we present results on shift-dependent measure of ECE and its dynamic past version. These results contain stochastic order, upper and lower bounds, the symmetry property and some relationships with other reliability functions. We also discuss some properties of conditional weighted ECE under some assumptions. Finally, we propose a nonparametric estimator of this new measure and study its practical results in blind image quality assessment.

Keywords: extended cumulative entropy; image quality assessment; past lifetime; Rényi entropy

1. Introduction

Differential entropy is a basic concept in the field of information theory. The central idea of information theory revolves around the concept of uncertainty introduced by Shannon [1]. If X is a random variable representing the lifetime of a system with probability density function (PDF) f, then the Shannon entropy of X is given by

$$H(X) = -\int_0^{+\infty} f(x) \log f(x) dx. \tag{1}$$

Later, Rényi [2] introduced another extension of the Shannon entropy that is more flexible than Shannon entropy and has a wide range of applications in many fields. The Rényi entropy of X, which we denote by $H_\alpha(X)$, is defined as follows:

$$H_\alpha(X) = \frac{1}{1-\alpha} \log \int_0^{+\infty} f^\alpha(x), \quad \alpha > 0 \ (\alpha \neq 1). \tag{2}$$

By replacing the PDF by the survival function $\bar{F} = 1 - F$ in (1), Rao et al. [3] defined an alternate information measure called the cumulative residual entropy (CRE) given by

$$\mathcal{E}(X) = \int_0^{+\infty} \bar{F}(x) \Lambda(x) dx,$$

where $\Lambda(x) = -\log \bar{F}(x)$. Di Crescenzo and Longobardi [4] introduced a new information measure similar to $\mathcal{E}(X)$ as follows:

$$\mathcal{CE}(X) = \int_0^{+\infty} F(x)\tilde{\Lambda}(x)dx, \tag{3}$$

where $\tilde{\Lambda}(x) = -\log F(x)$. Recently Di Crescenzo and Toomaj [5] discussed some properties of a new weighted distribution based on a cumulative entropy (CE) function. Psarrakos and Navarro [6] generalized the concept of CRE, relating this concept with the mean time between record values and with the concept of relevation transform, and also considered a dynamic version of this new measure (for more details see Calí, Longobardi and Psarrakos, [7]). Moharana and Kayal [8] obtained some results on the weighted extended cumulative residual entropy of k-th upper record values. Tahmasebi et al. [9] considered a shift-dependent measure of generalized cumulative entropy and its dynamic version in the case where the weight is a general non-negative function. An important concept of ordered random variables which arises in many areas of applications is the concept of record values. Consider the sequence $\{X_n, n \geq 1\}$ of independent and identically distributed random variables with cumulative distribution function (CDF) F and PDF f. An observation X_j is called a lower record if $X_j < X_i$ for every $i < j$. For a fixed positive integer k, the sequence $\{L_{n(k)}, n \geq 1\}$ of k-th lower record times for $\{X_n, n \geq 1\}$ is defined by Dziubdziela and Kopocinski [10] as follows:

$$L_{1(k)} = 1, \quad L_{n+1(k)} = min\{j > L_{n(k)} : X_{k:L_{n(k)}+k-1} > X_{k:k+j-1}\},$$

where $X_{j:m}$ denotes the j-th order statistic in a sample of size m. Then $X_{n(k)} := X_{k:L_{n(k)}+k-1}$ is called a sequence of k-th lower record values of $\{X_n, n \geq 1\}$. Aditionally, the PDF and CDF of $X_{n(k)}$, which are denoted by $f_{n(k)}$ and $F_{n(k)}$, respectively, are given by

$$f_{n(k)}(x) = \frac{k^n}{(n-1)!}[F(x)]^{k-1}[\tilde{\Lambda}(x)]^{n-1}f(x), \tag{4}$$

$$F_{n(k)}(x) = [F(x)]^k \sum_{i=0}^{n-1} \frac{[k\tilde{\Lambda}(x)]^i}{i!}. \tag{5}$$

Now, if we define $\tilde{\mu}_{n,k}(x) = \int_0^{+\infty} F_{n(k)}(x)dx$, from (5) we obtain

$$k\,[\tilde{\mu}_{n+1,k}(x) - \tilde{\mu}_{n,k}(x)] = \int_0^{+\infty} \frac{k^{n+1}}{n!}[F(x)]^k[\tilde{\Lambda}(x)]^n dx. \tag{6}$$

Tahmasebi and Eskandarzadeh [11] defined a further extension of CE as follows:

$$\begin{aligned} \mathcal{CE}_{n,k}(X) &= \int_0^{+\infty} \frac{k^{n+1}}{n!}[F(x)]^k[\tilde{\Lambda}(x)]^n dx \\ &= \mathbb{E}\left(\frac{1}{r(X_{n+1(k)})}\right), \quad for \;\; n = 1,2,..., \;\; k \geq 1, \end{aligned} \tag{7}$$

where $r(.) = \frac{f(.)}{F(.)}$ is the reversed failure rate of F. This new CE is presented on the idea of GCRE introduced by Psarrakos and Navarro [6]. They named it extended cumulative entropy (ECE).

Non-reference image quality assessment (IQA) methods give quality estimates without prior knowledge of the reference image, and quality assessment is done based on the test images only. Image quality approaches largely depend on the intended imaging area. However, making an objective general quality assessment of image information based on a physical measurement of the image is interesting. Shannon entropy is classically used as a value to indicate the amount of uncertainty or information in a source. Quality and entropy are related issues. However, a barrier to entropy as the quality indicator is that it can't distinguish the noise of an image from the desired information. Hence, Shannon entropy is not a good indicator of image quality by itself. Overcoming this problem is presented by anisotropy as an appropriate measure of image quality. Degradation processes damage the directional scene's information. Hence, anisotropy, as a directionally dependent quality, is reduced by adding further damage to the image. Using neuroscience research, the local receptive field (LRF) in the primary visual cortex is highly adaptable to extract local features for visual comprehension, and simple cells in the LRF can be described as being used for localization and spatial orientation. In other words, the LRF is very sensitive to changes in intensity and orientation [12]. Therefore, visual information of an image can be represented by the local intensity and local orientation of the image. Thus, an image quality index must consider the local intensity and local orientation information of an image. The anisotropic quality index (AQI) uses R*é*nyi entropy as the basic criterion for the measuring of the image information content using the local intensity. For this purpose, as a first step the pseudo-winger distribution of the symmetric neighbors of each pixel at different directions is calculated. Then the R*é*nyi entropy of the obtained values is computed. Furthermore, AQI calculates the entropy at different directions in order to consider the local orientation information of an image. Although it seems that AQI considers the local intensity and local orientation information of an image for image quality estimation, R*é*nyi entropy only uses the distribution of the local intensity of pixels, and exact value of pixels are not used. Hence in this paper we propose a novel entropy measure which considers the distribution and exact value of pixels simultaneously. The results on three test images show the benefits of the proposed new measure of entropy. For this purpose, we present results on a shift-dependent measure of ECE and its dynamic past version. We also study the numerical results of ECE in blind image quality assessment. Therefore, the rest of this paper is organized as follows: In Section 2, we present some basic properties and the stochastic ordering of a weighted ECE (denoted by WECE). We also obtain some results from the dynamic version of the WECE. In Section 3, we study some properties of the conditional WECE. In Section 4, we state some relationships of the WECE with other concepts of reliability functions. Finally, in Section 5, using the nonparametric estimator of WECE, numerical results of a blind image quality assessment are presented.

2. Some Results on WECE and Its Dynamic Past Version

In this section, we first present some properties of the WECE and then consider the dynamic past version of this concept.

Definition 1. *Let X be a non-negative random variable with CDF F. Then, the WECE is defined as follows:*

$$\begin{aligned} \mathcal{CE}^{w}_{n,k}(X) &= \int_0^{+\infty} \frac{k^{n+1}}{n!} x[F(x)]^k[\tilde{\Lambda}(x)]^n dx \\ &= \mathbb{E}\left(\frac{X_{n+1(k)}}{r(X_{n+1(k)})}\right). \end{aligned} \tag{8}$$

Furthermore, from (5) we can obtain an alternative expression as

$$\mathcal{CE}^{w}_{n,k}(X) = \int_0^{+\infty} kx[F_{n+1(k)}(x) - F_{n(k)}(x)]dx.$$

Remark 1. *Let X be a non-negative absolutely continuous random variable:*

i. *If X is uniformly distributed in $[0,\theta]$, then, $\mathcal{CE}^{w}_{n,k}(X) = \theta^2(\frac{k}{k+2})^{n+1}$.*
ii. *If X has the Fréchet distribution with $F(x) = e^{\frac{-\theta}{x}}$, then for $n > 2$ we have*

$$\mathcal{CE}^{w}_{n,k}(X) = \frac{k^3\theta^2}{n(n-1)(n-2)} = k^3\mathcal{CE}^{w}_{n,1}(X).$$

iii. *If X has an inverse Weibull distribution with $F(x) = \exp(-(\frac{\alpha}{x})^{\beta})$, $\alpha, \beta > 0$, then $\mathcal{CE}^{w}_{n,k}(X) = \frac{\alpha^2 k^{\frac{\beta+2}{\beta}}}{\beta n!}\Gamma(\frac{n\beta-2}{\beta})$.*

iv. *If $Y = aX + b$, with $a > 0$ and $b \geq 0$, then $\mathcal{CE}^{w}_{n,k}(Y) = a^2\mathcal{CE}^{w}_{n,k}(X) + ab\mathcal{CE}_{n,k}(X)$.*

In the following, we prove important properties of the WECE using stochastic ordering. For that we present the following definition:

Definition 2. *Let X and Y be the non-negative random variables with CDFs F and G, respectively, then*

1. *X is smaller than Y in the usual stochastic order (denoted by $X \leq_{st} Y$) if $P(X \geq x) \leq P(Y \geq x)$ for all x.*
2. *X is smaller than Y in the likelihood ration ordering (denoted by $X \leq_{lr} Y$) if $\frac{f_Y(x)}{f_X(x)}$ is increasing in x;*
3. *X is smaller than Y in the reversed hazard rate order, denoted by $X \leq_{rhr} Y$, if $r_X(x) \geq r_Y(x)$ for all x;*
4. *X is smaller than Y in the decreasing convex order, denoted by $X \leq_{dcx} Y$, if $\mathbb{E}(\phi(X)) \leq \mathbb{E}(\phi(Y))$ for all decreasing convex functions ϕ such that the expectations exist;*
5. *X is smaller than Y in the dispersive order, denoted by $X \leq_{disp} Y$, if $F^{-1}(v) - F^{-1}(u) \leq G^{-1}(v) - G^{-1}(u)$, $\forall\ 0 < u \leq v < 1$, where F^{-1} and G^{-1} are right continuous inverses of F and G, respectively;*
6. *A non-negative random variable X is said to have a decreasing reversed hazard rate (DRHR) if $r_X(x) = \frac{f(x)}{F(x)}$ is decreasing in x;*
7. *A non-negative random variable X is said to have a decreasing reversed hazard rate average (DRHRA) if $\frac{r_X(x)}{x}$ is a decreasing function in $x > 0$. Note that DRHR classes of distributions are included in DRHRA classes of distributions.*

Theorem 1. *Let X be an absolutely continuous non-negative random variable with CDF F. If X is DRHRA, then*

$$\mathcal{CE}^{w}_{n+1,k}(X) \leq \mathcal{CE}^{w}_{n,k}(X), \quad \text{for} \ \ n = 1, \dots, \quad k \geq 1. \tag{9}$$

Proof. Since the ratio $\frac{f_{n+1(k)}(x)}{f_{n+2(k)}(x)} = \frac{-(n+1)}{k \log F(x)}$ is increasing in x, it follows that $X_{n+2(k)} \leq_{st} X_{n+1(k)}$. This is equivalent (Shaked and Shanthikumar [13], (p. 4)) to having

$$\mathbb{E}(\phi(X_{n+2(k)})) \leq \mathbb{E}(\phi(X_{n+1(k)})),$$

for all increasing functions ϕ such that these expectations exist. Hence, if X is DRHRA and r_X is its reversed hazard rate, then we have

$$\mathbb{E}\left(\frac{X_{n+2(k)}}{r_X(X_{n+2(k)})}\right) \leq \mathbb{E}\left(\frac{X_{n+1(k)}}{r_X(X_{n+1(k)})}\right),$$

and this completes the proof. □

Remark 2. *Assume that the non-negative random variable X is DRHRA, then we have*

$$\mathcal{CE}^{w}_{n,k}(X) \leq \mathcal{CE}^{w}_{n,k+1}(X), \quad \text{for} \ \ n = 1, \dots, \quad k \geq 1. \tag{10}$$

Remark 3. *Let X and Y be two non-negative random variables with finit functions $\mathcal{CE}^{w}_{n,k}(X)$ and $\mathcal{CE}^{w}_{n,k}(Y)$, respectively. If $X \leq_{rhr} Y$ and $\frac{x}{r_X(x)}$ is an increasing function of x, then*

$$\mathcal{CE}^{w}_{n,k}(X) \leq \mathcal{CE}^{w}_{n,k}(Y). \tag{11}$$

Proposition 1. *Let X and Y be non-negative random variables with CDFs F and G, respectively. If $X \leq_{disp} Y$, then we have*

$$\mathcal{CE}^{w}_{n,k}(X) \leq \mathcal{CE}^{w}_{n,k}(Y). \tag{12}$$

Proof. See Lemma 3 in Klein et al. [14]. □

Proposition 2. *Let X and Y be two independent non-negative random variables with distribution functions F and G, respectively. If X and Y have log-concave densities, then*

$$\mathcal{CE}^{w}_{n,k}(X+Y) \geq max\left\{\mathcal{CE}^{w}_{n,k}(X), \mathcal{CE}^{w}_{n,k}(Y)\right\}. \tag{13}$$

Proof. See Theorem 3.2 of Di Crescenzo and Toomaj [5]. □

Proposition 3. *Let X be a non-negative absolutely continuous random variable with CDF F. Then,*

$$\mathcal{CE}^{w}_{n,k}(X) \geq \sum_{i=0}^{n} \frac{(-1)^i k^{n+1}}{i!(n-i)!} \int_0^{+\infty} x[F(x)]^{i+k} dx.$$

Proof. The proof is similar to that Proposition 4.3 of Di Crescenzo and Longobardi [4]. □

Proposition 4. *Let X be a non-negative random variable with CDF F, then for any $k \geq 1$ we have*

$$\mathcal{CE}^{w}_{n,k}(X) \leq k^{n+1}\mathcal{CE}^{w}_{n}(X),$$

where $\mathcal{CE}^{w}_{n}(X)$ is the shift-dependent GCE of order n (see Kayal and Moharana [15]).

Assume that X and Y are the lifetimes of two components of a system with joint distribution function $F(x,y)$. Then the bivariate WECE can be defined as

$$\mathcal{CE}^{w}_{n,k}(X,Y) \quad = \quad \frac{k^{n+1}}{n!} \int_0^{+\infty} \int_0^{+\infty} xy[F(x,y)]^k [\tilde{\Lambda}(x,y)]^n dx\, dy, \tag{14}$$

where $\tilde{\Lambda}(x,y) = -\log F(x,y)$. Using the binomial expansion in (14), we obtain the following proposition.

Proposition 5. *Let X and Y be the independent random variables with joint distribution function $F(x,y)$, then using the symmetry property we have*

$$\mathcal{CE}^{w}_{n,k}(X,Y) = \frac{1}{k}\sum_{i=0}^{n} \mathcal{CE}^{w}_{n-i,k}(X)\mathcal{CE}^{w}_{i,k}(Y) = \frac{1}{k}\sum_{i=0}^{n} \mathcal{CE}^{w}_{i,k}(X)\mathcal{CE}^{w}_{n-i,k}(Y).$$

Suppose that X ia a random lifetime of a system with CDF F, then we state that $X_{[t]} = (t - X \mid X < t)$ describes the inactivity time of the system. Analogously, we can also consider the dynamic past version of WECE for $X_{[t]}$ as

$$\mathcal{CE}^{w}_{n,k}(X;t) = \int_0^t \frac{k^{n+1}}{n!} x \left[\frac{F(x)}{F(t)}\right]^k [\tilde{\Lambda}(x) - \tilde{\Lambda}(t)]^n dx\,, t > 0, \tag{15}$$

for $n = 1, 2, \ldots$, and $k \geq 1$. This function is called a weighted dynamic extension cumulative entropy (WDECE).

Proposition 6. *Let X be a non-negative absolutely continuous random variable with CDF F. Then,*

i. $\mathcal{CE}^{w}_{n,k}(X;\infty) = \mathcal{CE}^{w}_{n,k}(X)$.

ii.

$$\mathcal{CE}^{w}_{n,k}(X;t) = \frac{k^{n+1}}{[F(t)]^k} \sum_{i=0}^{n} \frac{(-1)^{n-i}}{i!(n-i)!} [\tilde{\Lambda}(t)]^{n-i} \int_0^t x[F(x)]^k [\tilde{\Lambda}(x)]^i dx. \tag{16}$$

iii.

$$\int_0^t x[F(x)]^k[\tilde{\Lambda}(x)]^n dx = \frac{n![F(t)]^k \mathcal{CE}^w_{n,k}(X;t)}{k^{n+1}} - \sum_{i=0}^{n-1}\binom{n}{i}(-1)^{n-i}[\tilde{\Lambda}(t)]^{n-i}\int_0^t x[F(x)]^k[\tilde{\Lambda}(x)]^i dx. \tag{17}$$

Proposition 7. *Suppose that the non-negative random variable X is DRHRA, then for $t > 0$ we have*

$$\mathcal{CE}^w_{n+1,k}(X;t) \le \mathcal{CE}^w_{n,k}(X;t) \quad \text{for} \quad n = 1, \dots, \quad k \ge 1.$$

Proof. We recall that if X is DRHRA, then $X_{[t]}$ is DRHRA and the proof follows from Theorem 1. □

Remark 4. *Assume that the non-negative random variable X is DRHRA, then we have*

$$\mathcal{CE}^w_{n,k}(X;t) \le \mathcal{CE}^w_{n,k+1}(X;t), \quad \text{for} \quad n = 1, \dots, \quad k \ge 1. \tag{18}$$

Theorem 2. *Let X be a non-negative absolutely continuous random variable with CDF F , then*

$$\frac{\partial}{\partial t}\mathcal{CE}^w_{n,k}(X;t) = kr(t)[\mathcal{CE}^w_{n-1,k}(X;t) - \mathcal{CE}^w_{n,k}(X;t)], \ t > 0. \tag{19}$$

Proof. The proof is similar to that Theorem 4 of Tahmasebi et al. [9]. □

Proposition 8. *Let X be a non-negative random variable with CDF F, then we have*

$$\mathcal{CE}^w_{n,1}(X;t) = \frac{\int_0^t \mathcal{CE}^w_{n-1,1}(X;x)f(x)dx}{F(t)} = \mathbb{E}[\mathcal{CE}^w_{n-1,1}(X;X) \mid X < t], \ t > 0.$$

Proposition 9. *Suppose that the non-negative random variable X is DRHRA, then $\mathcal{CE}^w_{n,k}(X;t)$ is increasing in $t > 0$ for $n = 1, 2, ...$ and $k \ge 1$.*

Definition 3. *We state that the non-negative random variable X has an increasing WDECE of order n (denoted by $IWDECE_n$) if $\mathcal{CE}^w_{n,k}(X;t)$ is increasing in t.*

Remark 5. *Let X be a non-negative random variable with CDF F. If X is DRHRA, then it is $IWDECE_n$ for $n = 1, 2, \dots$ and $k \ge 1$.*

Proposition 10. *For $k = 1$, if X is $IWDECE_{n-1}$, then it is $IWDECE_n$.*

Proof. Suppose that X is $IWDECE_{n-1}$. Then, by recalling Proposition 8 we have

$$\begin{aligned} \mathcal{CE}^w_{n,1}(X;t) &= \frac{\int_0^t \mathcal{CE}^w_{n-1,1}(X;x)f(x)dx}{F(t)} \\ &\le \frac{\int_0^t \mathcal{CE}^w_{n-1,1}(X;t)f(x)dx}{F(t)} = \mathcal{CE}^w_{n-1,1}(X;t). \end{aligned}$$

Furthermore, (19) implies that $\frac{\partial}{\partial t}\mathcal{CE}^w_{n,1}(X;t) \ge 0$ and X is $IWDECE_n$. □

3. Properties of Conditional WECE

Let X be a random variable on a probability space $(\Omega, \mathcal{F}, P)$ such that $\mathbb{E}|X| < \infty$. We denote by $\mathbb{E}(X|\mathcal{G})$ the conditional expectation of X given sub σ-field $\mathcal{G}$, where $\mathcal{G} \subset \mathcal{F}$. Here, we define the conditional WECE and discuss some of its properties.

Definition 4. *Suppose that X is a non-negative random variable with CDF F. Then for a given σ-field $\mathcal{F}$, the conditional WECE is defined as follows:*

$$\begin{aligned} \mathcal{CE}^w_{n,k}(X|\mathcal{F}) &= \frac{k^{n+1}}{n!} \int_{\mathbb{R}^+} x[\mathbb{P}(X \le x|\mathcal{F})]^k [-\log(\mathbb{P}(X \le x|\mathcal{F}))]^n dx \\ &= \frac{k^{n+1}}{n!} \int_{\mathbb{R}^+} x \left(\mathbb{E}[I_{(X\le x)}|\mathcal{F}]\right)^k [-\log(\mathbb{E}[I_{(X\le x)}|\mathcal{F}])]^n dx. \end{aligned}$$

Lemma 1. *Suppose that X is a non-negative random variable with CDF F. If $\mathcal{F} = \{\phi, \Omega\}$, then $\mathcal{CE}^w_{n,k}(X|\mathcal{F}) = \mathcal{CE}^w_{n,k}(X)$.*

Proposition 11. *Let $X \in L^p$ for some $p > 2$, then for $\sigma-$ fields $\mathcal{G} \subset \mathcal{F}$ we have*

$$\mathbb{E}(\mathcal{CE}^w_{n,k}(X|\mathcal{F})|\mathcal{G}) \le \mathcal{CE}^w_{n,k}(X|\mathcal{G}). \tag{20}$$

Proof. The proof follows by applying Jensen's inequality for the convex function $x^k(-logx)^n$, $0 < x < 1$ as

$$\begin{aligned} \mathbb{E}(\mathcal{CE}^w_n(X|\mathcal{F})|\mathcal{G}) &= \frac{k^{n+1}}{n!} \int_{\mathbb{R}^+} x\mathbb{E}\left[(\mathbb{P}(X \le x|\mathcal{F}))^k [-\log \mathbb{P}(X \le x|\mathcal{F})]^n |\mathcal{G}\right] dx \\ &\le \frac{k^{n+1}}{n!} \int_{\mathbb{R}^+} x \left(\mathbb{E}[\mathbb{E}(I_{(X\le x)}|\mathcal{F})|\mathcal{G}]\right)^k [-\log \mathbb{E}[\mathbb{E}(I_{(X\le x)}|\mathcal{F})|\mathcal{G}]]^n dx \\ &= \frac{k^{n+1}}{n!} \int_{\mathbb{R}^+} x \left[\mathbb{E}(I_{(X\le x)}|\mathcal{G})\right]^k [-\log \mathbb{E}(I_{(X\le x)}|\mathcal{G})]^n dx, \end{aligned}$$

and the result follows. □

Lemma 2. *Let X, Y and Z be the non-negative random variables. If $X \to Y \to Z$ is a Markov chain, then we have*

i. $\mathcal{CE}^w_{n,k}(Z|Y, X) = \mathcal{CE}^w_{n,k}(Z|Y)$,
ii. $\mathbb{E}[\mathcal{CE}^w_{n,k}(Z|Y)] \le \mathbb{E}[\mathcal{CE}^w_{n,k}(Z|X)]$.

Proof.

(i) By using the Markov property and definition of $\mathcal{CE}^w_{n,k}(Z|Y, X)$, the result follows.
(ii) Let $\mathcal{G} = \sigma(X)$ and $\mathcal{F} = \sigma(X, Y)$, then from (20) we have

$$\begin{aligned} \mathbb{E}[\mathcal{CE}^w_{n,k}(Z|X)] &\ge \mathbb{E}(\mathbb{E}[\mathcal{CE}^w_{n,k}(Z|X, Y)|X]) \\ &= \mathbb{E}[\mathcal{CE}^w_{n,k}(Z|X, Y)] \\ &= \mathbb{E}[\mathcal{CE}^w_{n,k}(Z|Y)], \end{aligned}$$

and the result follows.

□

Theorem 3. *Let $X \in L^p$ for some $p > 2$ be a non-negative random variable with CDF F and $\mathcal{F}$ be a $\sigma-$ field. Then $\mathbb{E}(\mathcal{CE}^w_{n,k}(X|\mathcal{F})) = 0$ if X is $\mathcal{F}$-measurable.*

Proof. Let $\mathbb{E}(\mathcal{CE}^{w}_{n,k}(X|\mathcal{F})) = 0$, then $\mathcal{CE}^{w}_{n,k}(X|\mathcal{F}) = 0$. By using the definition of $\mathcal{CE}^{w}_{n,k}(X|\mathcal{F})$ we conclude that $\mathbb{E}(I_{(X\leq x)}|\mathcal{F}) = 0$ or 1. Thus, using the relation (24) of Rao et al. [3], X is $\mathcal{F}$-measurable. Supposing that X is $\mathcal{F}$-measurable, again using relation (24) of Rao et al. [3], we have $P(X \leq x|\mathcal{F}) = 0$ or 1 for almost all $x \in \mathbb{R}^{+}$, thus the result follows. □

Theorem 4. *Let X be a non-negative random variable with CDF F and $\mathcal{F}$ be a $\sigma-$ field, then we have*

$$\mathbb{E}(\mathcal{CE}^{w}_{n,k}(X|\mathcal{F})) \leq \mathcal{CE}^{w}_{n,k}(X), \tag{21}$$

and the equality holds if, and only if, X is independent of $\mathcal{F}$.

Proof. The inequality (21) follows from (20) by taking $\mathcal{F} = \{\phi, \Omega\}$. Assume that X is independent of $\mathcal{F}$, then clearly

$$\mathbb{P}(X \leq x \mid \mathcal{F}) = \mathbb{P}(X \leq x). \tag{22}$$

By using Definition 4 and (20), we have

$$\mathbb{E}(\mathcal{CE}^{w}_{n,k}(X|\mathcal{F})) = \mathcal{CE}^{w}_{n,k}(X).$$

Conversely, suppose that there is equality in (21). We put $W := \mathbb{P}(X \leq x \mid \mathcal{F})$; since $\varphi(w) = w^{k}[-\log w]^{n}$ is strictly convex and $\mathbb{E}[\varphi(W)] = \varphi[\mathbb{E}(W)]$, then we have $\mathbb{P}(X \leq x \mid \mathcal{F}) = \mathbb{P}(X \leq x)$, i.e., X is independent of $\mathcal{F}$. □

4. Relationships with Other Reliability Functions

In this section, we state some relationships of $\mathcal{CE}^{w}_{n,k}(X)$ and $\mathcal{CE}^{w}_{n,k}(X;t)$ with other concepts such as the reversed hazard rate function and the weighted mean inactivity time of the random variable $[t - X_{n(k)} \mid X_{n(k)} < t]$.

Theorem 5. *Let X be an absolutely continuous non-negative random variable with PDF f and CDF F. Then for $n \geq 1$ we have*

$$\mathcal{CE}^{w}_{n,k}(X) = \frac{k^{n+1}}{n!}\int_{0}^{+\infty} r(z)\left\{\int_{0}^{z} x[F(x)]^{k}[\tilde{\Lambda}(x)]^{n-1}dx\right\}dz. \tag{23}$$

Proof. By (8) and the relation $\tilde{\Lambda}(x) = \int_{x}^{\infty} r(z)dz$, we have

$$\mathcal{CE}^{w}_{n,k}(X) = \frac{k^{n+1}}{n!}\int_{0}^{+\infty}\int_{x}^{\infty} r(z)x[F(x)]^{k}[\tilde{\Lambda}(x)]^{n-1}dzdx.$$

Using Fubini's theorem, we obtain

$$\mathcal{CE}^{w}_{n,k}(X) = \frac{k^{n+1}}{n!}\int_{0}^{+\infty}\int_{0}^{z} r(z)x[F(x)]^{k}[\tilde{\Lambda}(x)]^{n-1}dxdz,$$

and the result follows.

Now, we define the weighted mean inactivity time of the random variable $[t - X_{n(k)} \mid X_{n(k)} < t]$ as follows:

$$\tilde{M}^{w}_{n,k}(t) = \frac{\sum_{j=0}^{n-1}\int_{0}^{t}\frac{k^{j}}{j!}x[F(x)]^{k}[\tilde{\Lambda}(x)]^{j}dx}{\sum_{j=0}^{n-1}\frac{k^{j}}{j!}[F(t)]^{k}[\tilde{\Lambda}(t)]^{j}}. \tag{24}$$

$\tilde{M}^{w}_{n,k}(t)$ is analogous to the mean residual waiting time used in reliability analysis (Bdair and Raqab [16]). □

Theorem 6. *For a non-negative absolutely continuous random variable X with $\mathcal{CE}^{w}_{n,k}(X) < \infty$, we have*

$$\mathcal{CE}^{w}_{n,k}(X) = \frac{1}{n}\sum_{j=0}^{n-1}[k\mathbb{E}[\tilde{M}^{w}_{n,k}(X_{(j+1)k})] - j\mathcal{CE}^{w}_{j,k}(X)].$$

Proof. From relation (23) and (24), we get

$$\begin{aligned}\sum_{j=1}^{n} j\mathcal{CE}^{w}_{j,k}(X) &= \int_0^{+\infty} r(z)\sum_{j=1}^{n}\int_0^z \frac{k^{j+1}}{(j-1)!}x[F(x)]^k[\tilde{\Lambda}(x)]^{j-1}dxdz \\ &= \int_0^{+\infty} r(z)\sum_{j=0}^{n-1}\int_0^z \frac{k^{j+2}}{j!}x[F(x)]^k[\tilde{\Lambda}(x)]^{j}dxdz \\ &= \int_0^{+\infty} r(z)k^2\tilde{M}^{w}_{n,k}(z)\left[\sum_{j=0}^{n-1}\frac{k^j}{j!}[F(z)]^k[\tilde{\Lambda}(z)]^j\right]dz \\ &= k\sum_{j=0}^{n-1}\mathbb{E}[\tilde{M}^{w}_{n,k}(X_{(j+1)k})],\end{aligned}$$

and this completes the proof. □

From (24), we can obtain the following result as

$$\tilde{M}^{w}_{n,k}(t) = \sum_{j=0}^{n-1} Z^{w}_{j,k}(t)q_{j,k}(t), \tag{25}$$

where

$$Z^{w}_{j,k}(t) = \int_0^t k^j x\left[\frac{F(x)}{F(t)}\right]^k\left[\frac{\tilde{\Lambda}(x)}{\tilde{\Lambda}(t)}\right]^j dx \tag{26}$$

and

$$q_{j,k}(t) = \frac{\frac{[\tilde{\Lambda}(t)]^j}{j!}}{\sum_{i=0}^{n-1}\frac{k^i[\tilde{\Lambda}(t)]^i}{i!}}. \tag{27}$$

To obtain a connection between $\tilde{M}^{w}_{n,k}(t)$ and $\mathcal{CE}^{w}_{n,k}(X;t)$ we need the following lemma.

Lemma 3. *Let X be a non-negative random variable with CDF F. Then we have*

$$Z^{w}_{j,k}(t) = \sum_{i=0}^{j}\frac{j!}{(j-i)!}\frac{k^{j-i-1}}{[\tilde{\Lambda}(t)]^i}\mathcal{CE}^{w}_{i,k}(X;t). \tag{28}$$

Proof. From (26), we have

$$
\begin{aligned}
Z^{w}_{j,k}(t) &= \int_0^t k^j x \left[\frac{F(x)}{F(t)}\right]^k \left[\frac{-\log(\frac{F(x)}{F(t)})}{\tilde{\Lambda}(t)} + 1\right]^j dx \\
&= \sum_{i=0}^{j} \frac{j!}{(j-i)!} \frac{k^{j-i-1}}{[\tilde{\Lambda}(t)]^i} \int_0^t \frac{k^{i+1}}{i!} \left[-\log\left(\frac{F(x)}{F(t)}\right)\right]^i x \left[\frac{F(x)}{F(t)}\right]^k dx \\
&= \sum_{i=0}^{j} \frac{j!}{(j-i)!} \frac{k^{j-i-1}}{[\tilde{\Lambda}(t)]^i} \mathcal{CE}^{w}_{i,k}(X;t).
\end{aligned}
$$

In the following, we can obtain the connection between $\tilde{M}^{w}_{n,k}(t)$ and $\mathcal{CE}^{w}_{n,k}(X;t)$. □

Theorem 7. *Let X be a non-negative random variable with CDF F, then for $n \geq 1$ we have*

$$
\tilde{M}^{w}_{n,k}(t) = \sum_{i=0}^{n-1} \mathcal{CE}^{w}_{i,k}(X;t)\eta_{i,k}(t),
$$

where

$$
\eta_{i,k}(t) = \frac{\sum_{j=0}^{n-i} \frac{k^{j-1}[\tilde{\Lambda}(t)]^j}{j!}}{\sum_{l=0}^{n-1} \frac{k^l[\tilde{\Lambda}(t)]^l}{l!}}, \quad i = 0, 1, ..., n.
$$

Proof. By (25) and (28), we have

$$
\begin{aligned}
\tilde{M}^{w}_{n,k}(t) &= \sum_{i=0}^{n-1} \sum_{j=i}^{n-1} \frac{j!}{(j-i)!} \frac{k^{j-i-1}}{[\tilde{\Lambda}(t)]^i} \mathcal{CE}^{w}_{i,k}(X;t) q_{j,k}(t) \\
&= \sum_{i=0}^{n-1} \mathcal{CE}^{w}_{i,k}(X;t) \frac{\sum_{j=i}^{n-1} \frac{k^{j-i-1}[\tilde{\Lambda}(t)]^{j-i}}{(j-i)!}}{\sum_{l=0}^{n-1} \frac{k^l[\tilde{\Lambda}(t)]^l}{l!}} \\
&= \sum_{i=0}^{n-1} \mathcal{CE}^{w}_{i,k}(X;t) \frac{\sum_{j=0}^{n-i} \frac{k^{j-1}[\tilde{\Lambda}(t)]^j}{j!}}{\sum_{l=0}^{n-1} \frac{k^l[\tilde{\Lambda}(t)]^l}{l!}},
\end{aligned}
$$

and this completes the proof. □

Theorem 8. *Let X be a non-negative random variable with CDF F, then for any $n \geq 1$ we have*

$$
\begin{aligned}
\mathcal{CE}^{w}_{n,k}(X) &= \frac{1}{n} \sum_{i=0}^{n-1} \frac{k^{i+2}}{i!} \mathbb{E}([F(X)]^{k-1}[\tilde{\Lambda}(X)]^i \tilde{M}^{w}_{n,k}(X)) \\
&- \frac{1}{n} \sum_{i=0}^{n-2} \frac{k^{i+2}}{i!} \mathbb{E}([F(X)]^{k-1}[\tilde{\Lambda}(X)]^i \tilde{M}^{w}_{n-1,k}(X)),
\end{aligned} \tag{29}
$$

where

$$
\tilde{M}^{w}_{n,k}(t) = \frac{1}{F_{n(k)}(t)} \int_0^t x F_{n(k)}(x) dx, \quad n = 1, 2, 3, ...
$$

is the weighted mean inactivity time of $X_{n(k)}$.

Proof. From (5), we see that

$$F_{n(k)}(t) - F_{n-1(k)}(t) = \frac{[k\tilde{\Lambda}(t)]^{n-1}}{(n-1)!}[F(t)]^k.$$

Substituting this equation in (23) we have

$$\begin{aligned}
\mathcal{CE}^w_{n,k}(X) &= \frac{k^2}{n}\int_0^{+\infty} r(z)\left\{\int_0^z x[F_{n(k)}(x) - F_{n-1(k)}(x)]dx\right\}dz \\
&= \frac{k^2}{n}\int_0^{+\infty} f(z)\left\{\frac{F_{n(k)}(z)}{F(z)}\tilde{M}^w_{n,k}(z) - \frac{F_{n-1(k)}(z)}{F(z)}\tilde{M}^w_{n-1,k}(z)\right\}dz \\
&= \frac{k^2}{n}\int_0^{+\infty} f(z)[F(z)]^{k-1}\left\{\sum_{i=0}^{n-1}\frac{[k\tilde{\Lambda}(z)]^i}{i!}\tilde{M}^w_{n,k}(z) - \sum_{i=0}^{n-2}\frac{[k\tilde{\Lambda}(z)]^i}{i!}\tilde{M}_{n-1,k}(z)\right\}dz,
\end{aligned} \tag{30}$$

and the result follows. □

Remark 6. *For a non-negative absolutely continuous random variable X with $\mathcal{CE}^w_{n,k}(X) < \infty$, we have*

$$\mathcal{CE}^w_{n,k}(X) = \frac{k}{n}\left\{\sum_{i=0}^{n-1}\mathbb{E}\left(\tilde{M}^w_{n,k}(X_{i+1(k)})\right) - \sum_{i=0}^{n-2}\mathbb{E}\left(\tilde{M}^w_{n-1,k}(X_{i+1(k)})\right)\right\}. \tag{31}$$

5. Application of $\mathcal{CE}^w_{n,k}(X)$ in Blind Image Quality Assessment

Suppose that $X_1, X_2, ..., X_m$ is a random sample of size m from CDF $F(x)$. If $X_{(1)} \leq X_{(2)} \leq ... \leq X_{(m)}$ represent the order statistics of $X_1, X_2, ..., X_m$, then the empirical measure of $F(x)$ for $i = 1, 2, ..., m-1$ is defined as

$$\hat{F}_m(x) = \begin{cases} 0, & x < X_{(1)}, \\ \frac{i}{m}, & X_{(i)} \leq x < X_{(i+1)}, \\ 1, & x \geq X_{(m)}. \end{cases}$$

Thus the empirical measure of $\mathcal{CE}^w_{n,k}(X)$ is obtained as

$$\begin{aligned}
\mathcal{CE}^w_{n,k}(\hat{F}_m) &= \frac{k^{n+1}}{n!}\int_0^{+\infty} x[\hat{F}_m(x)]^k\left(-\log\hat{F}_m(x)\right)^n dx \\
&= \frac{k^{n+1}}{n!}\sum_{i=1}^{m-1}\sum_{j=0}^{n}(-1)^j\binom{n}{j}U_i\left(\frac{i}{m}\right)^k[\log i]^j[\log m]^{n-j},
\end{aligned} \tag{32}$$

where $U_i = \frac{X^2_{(i+1)} - X^2_{(i)}}{2}$. Note that $\mathcal{CE}^w_{n,k}(\hat{F}_m) \to \mathcal{CE}^w_{n,k}(F)$ as $m \to \infty$ (see Theorem 14 of Tahmasebi et al. [9]). In the following example we present applications of $\mathcal{CE}^w_{n,k}(\hat{F}_m)$ in blind image quality assessment.

Example 1 (Blind Image Quality Assessment). *In this example a modified anisotropic image quality (AIQ) measure based on the WECE is used as a blind image quality index, which we call WECE-AIQ. The old AIQ is based on the using of Rényi entropy and the normalized pseudo-Wigner distribution [17]. We call this measure Rényi-AIQ. Dataset [18,19] is used in this example for blind image quality assessment. The dataset contains distorted images of three grayscale reference images: a horse, a harbor and a baby (Figure 1). The size and pixel values of the images are* 512 × 512 *and in the range 0–255, respectively. The reference images are distorted using "flat allocation"; quantization of the LH sub-bands of a 5-level DWT of the image with equal distortion contrast at each scale (FLT), baseline JPEG compression (JPG), baseline JPEG-2000 compression (JP2), JPEG-2000+DCQ* *compression (DCQ), Gaussian blur filter (BLR) and additive Gaussian white noise (AGWN). These distortions are utilized to reference images in three levels: low quality (LQ), mid quality (MQ) and good quality (GQ). In this example, WECE is used instead of Rényi entropy for the estimation of the AIQ metric, and k and n are selected as 2 and 4 for WECE, respectively. For the assessment of the Rényi-AIQ and WECE-AIQ metrics, some full-reference image quality metrics are needed: PSNR, WSNR, a weighted SNR [20], a universal quality index (UQI) [21], a noise quality measure (NQM) [22], a structural similarity metric (SSIM) [23], a visual information fidelity (VIF) metric [24] and a visual SNR (VSNR) [18]. A bigger value of each of these metrics indicates a better quality of an image. The values of these metrics are available for images of the database used in this example [19]. Note that only gray scale images are considered in this example. For color images, only spatial structures cannot properly demonstrate the quality of an image. Visual damage caused by distortion of the image's color must be considered. Therefore, a criterion for color distortion must be used. The color image can be decomposed into different color spaces such as RGB, CIE, YCbCr, YIQ, HIS etc. [25]. LMN space, with the optimized weights that are suitable for the human visual system (HVS), can be a good choice [25]. L is the luminance channel for evaluating the structure distortions of the images, and M and N are two chrominance channels which are used to characterize the image quality degradation caused by color distortions. an image quality metric is applied on the L channel for structure distortions measurement and on the M and N channels for color distortions measurement. The values of Rényi-AIQ, WECE-AIQ and full-reference metrics are depicted in Table 1. The biggest value of Rényi-AIQ and WECE-AIQ metrics are shown using bold numbers for each image. The performance of WECE-AIQ and Rényi-AIQ is measured using the times in which a full-reference criterion of the selected image of each approach is larger than in the other approaches. It can be seen from Table 1 which WECE-AIQ displayed a better performance than Rényi-AIQ for the "Horse (GQ)", "Horse (LQ)", "Harbor (GQ)", "Harbor (MQ)" and "Harbor (LQ)" images. This shows that the quality of the selected images using the WECE-AIQ metric is better than the ones which were selected using the Rényi-AIQ metric. For visual analysis of the results of Table 1, corresponding images with the biggest values of Rényi-AIQ and WECE-AIQ metrics are shown in Figures 2–4. It can be seen that in most cases, the visual quality of images which were selected using the WECE-AIQ metric was higher than the ones which were chosen using Rényi-AIQ. For more analysis of the results of Table 1, Spearman's rank correlation coefficient (SRCC) was used in this example [26]. The results of this measure are shown in Table 2. Table 2 shows the SRCC between full-reference and blind image quality metrics for each image. Bold numbers show the bigger SRCC value of each full-reference metrics. In general, the Spearman's rank correlation coefficient range is* $[-1, 1]$*. In this example, each blind image quality metric that has a bigger Spearman's rank correlation coefficient value than others is more useful for image quality assessment. Table 2 shows that for all images, the performance of WECE-AIQ was better than Rényi-AIQ. Additionally, the performance of WECE-AIQ for the harbor image was better than for the horse and baby image. The corresponding SRCC values of WECE-AIQ for the harbor image were positive in most cases. This shows that the quality ranks of images, which are selected using WECE-AIQ, are very similar to the quality ranks of full-reference metrics. Hence it seems that WECE-AIQ has worked much more effectively than Rényi-AIQ on the harbor image. Indeed, none of the full-reference image quality metric had a high correlation with the HVS. The accuracy of each one depends on the distortion type, context and texture of the distorted image. Therefore in general, the quality of a distorted image is evaluated using some of the full-reference image quality criteria. For further investigation of this subject, the Spearman's rank correlation coefficients (SRCCs) between each of the full-reference criterions of the horse image are illustrated at Table 3. Contrary to what was expected, it is seen that the correlation between the full-reference criteria was not high in most cases. Additionally, as can be seen in Table 2, the correlation of Rényi-AIQ and WECE-AIQ with the full-reference image quality criteria was not high. This is due to the fact that each criterion evaluates the distorted image from a different point of view compared with the others. For example, PSNR calculates the difference between the distorted and reference images, while SSIM is based on the structural similarity between them. Indeed, none of the full-reference image quality criteria consider all of the properties of HVS. Therefore, in this research the performance of Rényi-AIQ and WECE-AIQ have been evaluated using the correlation between them and all of the full-reference image quality criteria.*

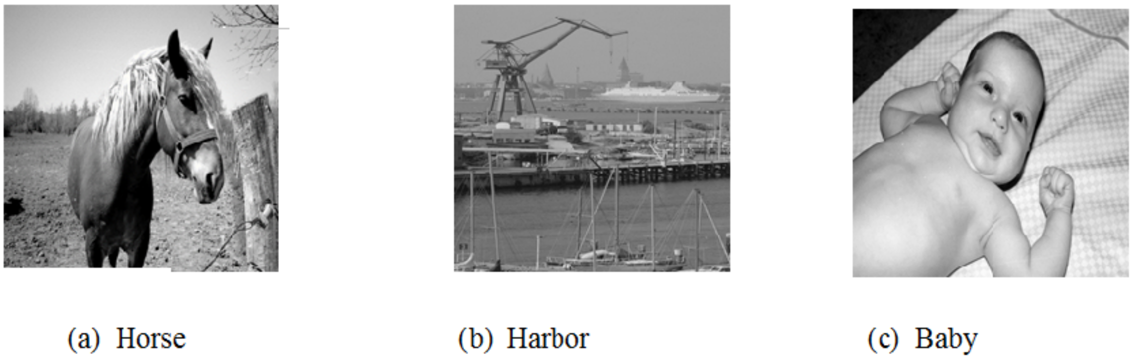

Figure 1. Referenecs of horse, harbor and baby images (**a**, **b** and **c**, respectively).

Figure 2. Best quality images that were selected using the R*é*nyi-AIQ metric from GQ, MQ and LQ distorted horse images (**a**, **c** and **e**, respectively), and best quality images that were selected using the WECE-AIQ metric from GQ, MQ and LQ distorted horse images (**b**, **d** and **f**, respectively).

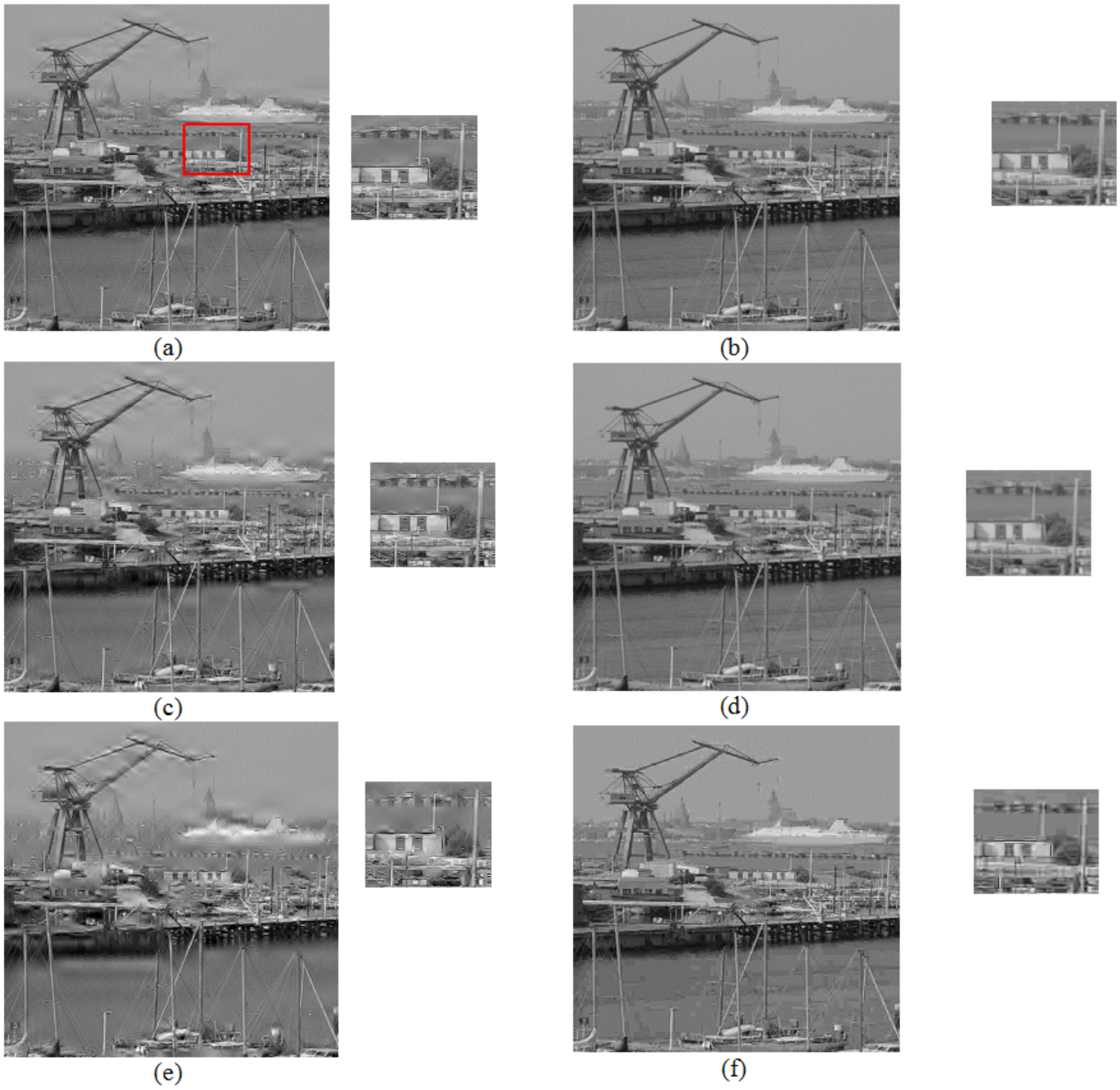

Figure 3. Best quality images that were selected using the R*é*nyi-AIQ metric from GQ, MQ and LQ distorted harbor images (**a**, **c** and **e**, respectively), and best quality images that were selected using the WECE-AIQ metric from GQ, MQ and LQ distorted harbor images (**b**, **d** and **f**, respectively).

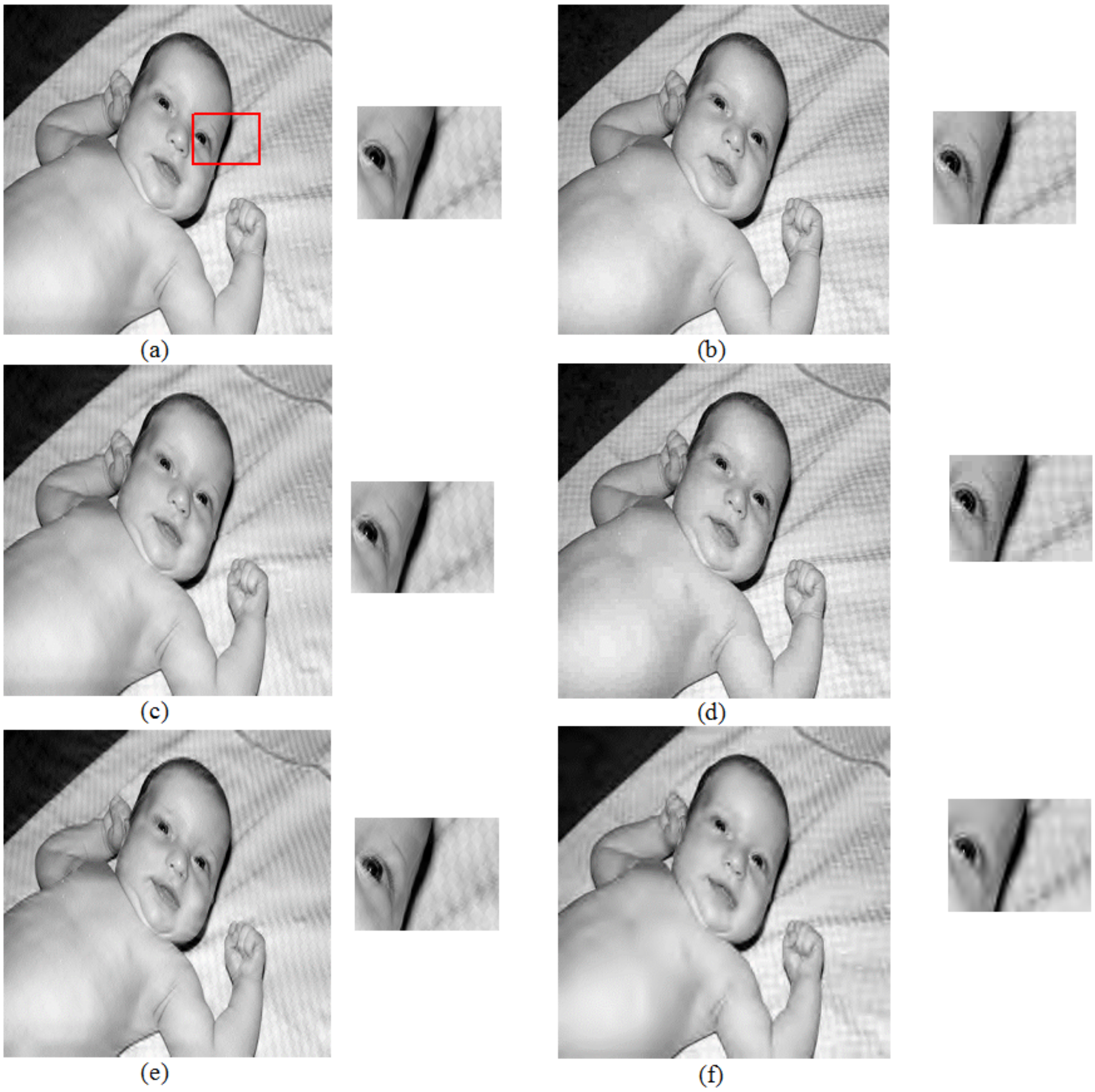

Figure 4. Best quality images that were selected using the Rényi-AIQ metric from GQ, MQ and LQ distorted baby images (**a**, **c** and **e**, respectively), and best quality images that were selected using the WECE-AIQ metric from GQ, MQ and LQ distorted baby images (**b**, **d** and **f**, respectively).

Table 1. Comparison of full-reference and blind image quality indexes.

Image	Distortion	Full-Reference Image Quality Metric						Blind Image Quality Metric	
		SSIM	VIF	NQM	UQI	PSNR	VSNR	Rényi-AIQ	WECE-AIQ
Horse (GQ)	FLT	0.933	0.570	19.391	0.833	28.983	20.597	0.00503661	0.00128575
	JPG	0.970	0.572	33.125	0.694	29.003	30.095	0.00564478	0.00114628
	JP2	0.946	0.427	30.446	0.656	28.870	27.700	0.0064663	0.00124661
	DCQ	0.962	0.508	31.849	0.685	28.891	36.342	0.00577385	0.00112959
	BLR	0.974	0.637	38.456	0.816	29.056	26.884	0.00565214	0.0013568
	AGWN	0.907	0.559	29.675	0.659	28.822	28.584	0.00399926	0.00072772

Table 1. *Cont.*

Image	Distortion	Full-Reference Image Quality Metric						Blind Image Quality Metric	
		SSIM	**VIF**	**NQM**	**UQI**	**PSNR**	**VSNR**	**Rényi-AIQ**	**WECE-AIQ**
Horse (MQ)	FLT	0.903	0.513	17.146	0.799	26.734	17.934	0.0054712	0.0011785
	JPG	0.926	0.374	28.033	0.589	26.701	23.736	0.0069904	0.0014497
	JP2	0.895	0.289	26.124	0.558	26.545	23.230	0.0057527	0.0013887
	DCQ	0.938	0.416	31.940	0.624	26.590	27.577	0.0052392	0.0013404
	BLR	0.944	0.498	34.419	0.702	26.733	22.566	0.0037091	0.0005268
	AGWN	0.861	0.473	27.612	0.603	26.496	25.518	0.0054970	0.0016277
Horse (LQ)	FLT	0.840	0.437	13.808	0.709	23.777	14.561	0.00652794	0.0017846
	JPG	0.786	0.176	19.448	0.400	23.622	17.092	0.00549665	0.0016539
	JP2	0.753	0.122	19.999	0.371	23.230	15.921	0.0070989	0.0014571
	DCQ	0.781	0.137	23.099	0.396	23.213	15.997	0.00697058	0.0012112
	BLR	0.835	0.262	25.978	0.487	23.725	16.456	0.00395791	0.0011317
	AGWN	0.777	0.363	24.709	0.513	23.300	21.530	0.00318548	0.0003756
Harbor (GQ)	FLT	0.935	0.608	14.953	0.772	31.098	18.362	0.00317073	0.00113086
	JPG	0.984	0.735	28.190	0.672	31.149	31.659	0.00302575	0.00103601
	JP2	0.949	0.493	24.223	0.585	31.118	24.349	0.00303644	0.00113519
	DCQ	0.975	0.649	26.711	0.663	31.202	35.532	0.00313986	0.00110450
	BLR	0.989	0.769	36.825	0.880	31.211	29.284	0.00226195	0.00151543
	AGWN	0.934	0.640	26.318	0.658	31.097	26.079	0.00287300	0.000939305
Harbor (MQ)	FLT	0.906	0.545	12.597	0.721	28.740	15.843	0.0031356	0.0010805
	JPG	0.968	0.589	26.207	0.608	28.909	26.549	0.00292496	0.00115297
	JP2	0.918	0.363	21.363	0.515	28.792	21.245	0.002908160	0.00111366
	DCQ	0.959	0.540	26.106	0.592	28.858	30.429	0.0030507	0.00119234
	BLR	0.979	0.684	35.112	0.784	28.908	25.740	0.00195757	0.001470153
	AGWN	0.895	0.552	24.244	0.607	28.724	23.095	0.00275998	0.001070499
Harbor (LQ)	FLT	0.854	0.462	9.254	0.651	25.556	12.315	0.00277902	0.00110425
	JPG	0.896	0.302	18.306	0.439	25.502	18.411	0.002717076	0.0014915792
	JP2	0.843	0.204	16.939	0.384	25.569	16.309	0.00231397	0.0010248261
	DCQ	0.931	0.395	24.526	0.490	25.610	27.498	0.002142166	0.0010449862
	BLR	0.939	0.490	30.010	0.576	25.802	19.524	0.001351146	0.0014994589
	AGWN	0.818	0.438	21.897	0.526	25.536	19.318	0.002607232	0.0005917831
Baby (GQ)	FLT	0.948	0.614	22.824	0.843	34.485	23.352	0.001806857	0.000464815
	JPG	0.955	0.504	29.818	0.718	34.528	27.700	0.001632599	0.000500301
	JP2	0.945	0.413	28.877	0.675	34.504	26.049	0.001734634	0.00034369
	DCQ	0.968	0.547	30.761	0.751	34.522	28.767	0.001640073	0.000445138
	BLR	0.979	0.637	34.323	0.824	34.636	26.431	0.001428632	0.000429976
	AGWN	0.963	0.716	32.966	0.732	34.564	31.574	0.00170072	0.000383635
Baby (MQ)	FLT	0.932	0.573	21.512	0.802	32.828	21.422	0.001849179	0.000506972
	JPG	0.919	0.376	26.591	0.630	32.738	24.065	0.001550735	0.000520883
	JP2	0.918	0.307	26.283	0.611	32.759	23.314	0.001649043	0.000329263
	DCQ	0.938	0.365	27.239	0.661	32.846	24.059	0.00159274	0.0003811
	BLR	0.964	0.530	30.984	0.769	32.931	23.131	0.001232089	0.00038633
	AGWN	0.946	0.647	31.594	0.665	32.740	29.220	0.001609792	0.000381473
Baby (LQ)	FLT	0.907	0.523	19.740	0.735	30.772	19.064	0.001757395	0.000498084
	JPG	0.859	0.264	22.941	0.507	30.722	20.583	0.001516522	0.001729756
	JP2	0.877	0.222	23.077	0.529	30.794	19.833	0.001483539	0.0046381869
	DCQ	0.915	0.283	26.433	0.613	30.803	19.935	0.001341795	0.0042625907
	BLR	0.935	0.402	26.743	0.688	31.012	19.711	0.000895241	0.003490746
	AGWN	0.916	0.561	30.352	0.581	30.740	26.674	0.001570303	0.000022357

Table 2. Spearman's rank correlation coefficient (SRCC) between full-reference and blind image quality metrics for each image.

Image	Blind Image Quality Index	Full-Reference Image Quality Metric					
		SSIM	VIF	NQM	UQI	PSNR	VSNR
Horse (GQ)	Rényi-AIQ	0.485	−0.428	0.42	−0.371	0.085	0.2
	WECE - AIQ	0.485	0.485	0.257	0.6	0.714	−0.771
Horse (MQ)	Rényi-AIQ	0.028	−0.485	−0.314	−0.257	0.028	−0.028
	WECE -AIQ	0.085	0.142	−0.485	0.314	0.485	−0.542
Horse (LQ)	Rényi-AIQ	−0.257	−0.657	−0.485	−0.657	−0.428	−0.771
	WECE -AIQ	0.428	0.028	−0.942	0.028	0.371	−0.657
Harbor (GQ)	Rényi-AIQ	−0.371	−0.714	−0.714	−0.314	−0.257	−0.257
	WECE -AIQ	0.485	−0.028	0.085	0.257	0.257	−0.257
Harbor (MQ)	Rényi-AIQ	−0.257	−0.485	−0.542	−0.142	−0.085	−0.085
	WECE -AIQ	0.942	0.314	0.771	0.257	0.828	0.657
Harbor (LQ)	Rényi-AIQ	−0.714	−0.2	−0.828	0.085	−0.257	−0.714
	WECE -AIQ	0.714	0.2	0.085	0.142	−0.028	−0.028
Baby (GQ)	Rényi-AIQ	−0.771	−0.142	−0.7714	0.028	−0.828	−0.428
	WECE -AIQ	−0.142	−0.2	−0.028	−0.6	0.085	0.657
Baby (MQ)	Rényi-AIQ	−0.485	0.085	−0.6	0.085	−0.2	−0.257
	WECE -AIQ	−0.085	−0.485	−0.028	−0.314	0.085	−0.028
Baby (LQ)	Rényi-AIQ	−0.371	0.428	−0.428	0.028	−0.771	0.085
	WECE -AIQ	0.314	0.314	−0.2	0.6	0.257	−0.542

Table 3. SRCC between full-reference image quality criteria of the horse image.

Image	Image Quality Index	Full-Reference Image Quality Index					
		SSIM	VIF	NQM	UQI	PSNR	VSNR
Horse (GQ)	SSIM	1	0.542857	0.942857	0.314286	0.828571	0.142857
	VIF	0.542857	1	0.485714	0.771429	0.828571	−0.31429
	NQM	0.942857	0.485714	1	0.085714	0.657143	0.314286
	UQI	0.314286	0.771429	0.085714	1	0.771429	−0.48571
	PSNR	0.828571	0.828571	0.657143	0.771429	1	−0.25714
	VSNR	0.142857	−0.31429	0.314286	−0.48571	−0.25714	1
Horse (MQ)	SSIM	1	0.2	0.771429	0.428571	0.6	−0.08571
	VIF	0.2	1	−0.02857	0.942857	0.6	−0.48571
	NQM	0.771429	−0.02857	1	0.085714	0.028571	0.371429
	UQI	0.428571	0.942857	0.085714	1	0.714286	−0.42857
	PSNR	0.6	0.6	0.028571	0.714286	1	−0.71429
	VSNR	−0.08571	−0.48571	0.371429	−0.42857	−0.71429	1
Horse (LQ)	SSIM	1	0.657143	−0.25714	0.657143	0.828571	−0.25714
	VIF	0.657143	1	−0.08571	1	0.771429	0.085714
	NQM	−0.25714	−0.08571	1	−0.08571	−0.25714	0.542857
	UQI	0.657143	1	−0.08571	1	0.771429	0.085714
	PSNR	0.828571	0.771429	−0.25714	0.771429	1	−0.14286
	VSNR	−0.25714	0.085714	0.542857	0.085714	−0.14286	1

6. Conclusions

In this paper, we have presented some results of the WECE and its dynamic past version. These results included stochastic ordering, bounds and some relationships with other reliability concepts.

Additionally, we examined the conditional WECE, which can be applied in measuring the uncertainty in blind image quality assessment. Finally, we proposed a nonparametric estimator of WECE and studied the numerical results of WECE in a blind image quality assessment. Furthermore, it can be seen that in most cases, the visual quality of images that were selected using the WECE-AIQ metric was higher than for images that were chosen using the R*é*nyi-AIQ metric. It was shown that the quality rank of images which are selected using the WECE-AIQ are very similar to the quality ranks of the full-reference metrics.

Author Contributions: All authors contributed equally to the manuscript. All authors have read and agreed to the published version of the manuscript.

Funding: This research received no external funding.

Acknowledgments: Maria Longobardi is partially supported by the GNAMPA research group of INDAM (Istituto Nazionale di Alta Matematica) and MIUR-PRIN 2017, Project "Stochastic Models for Complex Systems" (no. 2017JFFHSH).

Conflicts of Interest: The authors declare no conflict of interest.

References

1. Shannon, C.A. Mathematical theory of communication. *Bell Syst. Tech. J.* **1948**, *27*, 379–432. [CrossRef]
2. Renyi, A. On measures of entropy and information. In *Proceedings of the Fourth Berkeley Symposium on Mathematical Statistics and Probability*; University of California Press: Berkeley, CA, USA, 1961; pp. 547–561.
3. Rao, M.; Chen, Y.; Vemuri, B.C.; Wang, F. Cumulative Residual Entropy: A New Measure of Information. *IEEE Trans. Inf. Theory* **2004**, *50*, 1220–1228. [CrossRef]
4. Di Crescenzo, A.; Longobardi, M. On cumulative entropies. *J. Stat. Plan. Inference* **2009**, *139*, 4072–4087. [CrossRef]
5. Di Crescenzo, A.; Toomaj, A. Extension of the past lifetime and its connection to the cumulative entropy. *J. Appl. Probab.* **2015**, *52*, 1156–1174. [CrossRef]
6. Psarrakos, G.; Navarro, J. Generalized cumulative residual entropy and record values. *Metrika* **2013**, *76*, 623–640. [CrossRef]
7. Calì, C.; Longobardi, M.; Psarrakos, G. A family of weighted distributions based on the mean inactivity time and cumulative past entropies. *Ricerche di Matematica* **2019**. [CrossRef]
8. Moharana, R.; Kayal, S. On Weighted Extended Cumulative Residual Entropy of k-th Upper Record. In *Digital Business. Lecture Notes on Data Engineering and Communications Technologies*; Patnaik, S., Yang, X.S., Tavana, M., Popentiu-Vlădicescu, F., Qiao, F., Eds.; Springer: Cham, Switzerland, 2019; Volume 21.
9. Tahmasebi, S.; Longobardi, M.; Foroghi,F.; Lak, F. An extension of weighted generalized cumulative past measure of information. *Ricerche di Matematica* **2019**. [CrossRef]
10. Dziubdziela, W.; Kopocinski, B. Limiting properties of the k-th record value. *Zastos. Math.* **1976**, *15*, 187–190. [CrossRef]
11. Tahmasebi, S.; Eskandarzadeh, M. Generalized cumulative entropy based on kth lower record values. *Stat. Probab. Lett.* **2017**, *126*, 164–172. [CrossRef]
12. Olshausen, B.A.; Field, D.J. Emergence of simple-cell receptive field properties by learning a sparse code for natural images. *Nature* **1996**, *381*, 607. [CrossRef]
13. Shaked, M.; Shanthikumar, J.G. *Stochastic Orders*; Springer: New York, NY, USA, 2007.
14. Klein, I.; Mangold, B.; Doll, M. Cumulative paired ϕ-entropy. *Entropy* **2016**, *18*, 248. [CrossRef]
15. Kayal, S.; Moharana, S.R. A shift-dependent generalized cumulative entropy of order n. *Commun. Stat. Simul. Comput.* **2018**. [CrossRef]
16. Bdair, O.M.; Raqab, M.Z. Sharp upper bounds for the mean residual waiting time of records. *Statistics* **2012**, *46*, 69–84. [CrossRef]
17. Gabarda, S.; Cristobal, G. Blind image quality assessment through Anisotropy. *J. Opt. Soc. Am. A* **2007**, *24*, B42–B51. [CrossRef]
18. Chandler, D.M.; Hemami, S.S. VSNR: A Wavelet-Based Visual Signal-to-Noise Ratio for Natural Images. *IEEE Trans. Image Process.* **2007**, *16*, 2284–2298. [CrossRef]

19. Chandler, D.M.; Hemami, S.S. A57 Image Quality Database. 2018. Available online: http://vision.eng.shizuoka.ac.jp/mod/page/view.php?id=26 (accessed on 22 December 2019).
20. Mannos, J.L.; Sakrison, D.J. The effects of a visual fidelity criterion on the encoding of image. *IEEE Trans. Inf. Theory* **1974**, *IT-20*, 525–535. [CrossRef]
21. Wang, Z.; Bovik, A. A universal image quality index. *IEEE Signal Process. Lett.* **2002**, *9*, 81–84. [CrossRef]
22. Damera-Venkata, N.; Kite, T.D.; Geisler, W.S.; Evans, B.L.; Bovik, A.C. Image quality assessment based on a degradation model. *IEEE Trans. Image Process.* **2000**, *9*, 636–650. [CrossRef]
23. Wang, Z.; Bovik, A.; Sheikh, H.; Simoncelli, E. Image quality assessment: From error visibility to structural similarity. *IEEE Trans. Image Process.* **2004**, *13*, 600–612. [CrossRef]
24. Sheikh, H.R.; Bovik, A.C. Image information and visual quality. *IEEE Trans. Image Process.* **2006**, *15*, 430–444. [CrossRef]
25. Shi, Z.; Zhang, J.; Cao, Q.; Pang, K.; Luo, T. Full-reference image quality assessment based on image segmentation with edge feature. *Signal Process.* **2018**, *145*, 99–105. [CrossRef]
26. Fieller, E.C.; Hartley, H.O.; Pearson, E.S. Tests for rank correlation coefficients. I. *Biometrika* **1957**, *44*, 470–481. [CrossRef]